International Archives of Photogrammetry & Remote Sensing, 31(5):290-294, 1996

DIGITAL MONOPLOTTING AND PHOTO-UNWRAPPING OF DEVELOPABLE SURFACES IN ARCHITECTURAL PHOTOGRAMMETRY

G. E. Karras, P. Patias*, E. Petsa
Department of Surveying, National Technical University of Athens, GR–15780 Athens, Greece
*Department of Surveying, The Aristotle University of Thessaloniki, GR–54006 Thessaloniki, Greece

Commission V, Working Group 4

KEY WORDS: Monoplotting, Digital Surface Development, Image Transformation, Mosaic, Architecture

ABSTRACT

It is to the interest of both the photogrammetrist and the non-expert user that image-based measuring techniques and user-oriented packages applied to architectural and archaeological documentation be kept as simple as possible. In this context, the potential of single-image techniques should be exhausted, confining stereoscopic procedures to irregularly-shaped surfaces. This contribution discusses a monoscopic approach for regular 3D surfaces whose known analytical expression provides the missing equation. Products may be in both vector and raster forms obtained via monoplotting and orthoimaging, respectively. Further, in the cases of developable surfaces (e. g. circular cylinders) digital unwrapping of the original images can also be performed. Finally, the basic concept is tested with six non-metric photographs fully covering a small late-19th-centrury railway water-tower having the shape of a right circular cylinder. The unwinded plot of the surface as well as the mosaic of the digitally unwrapped images are presented.

1. INTRODUCTION

Documentation and conservation of cultural heritage are being increasingly seen as tasks of national – ultimately international – priority. Due to the digital techniques, photogrammetry now appears as more efficient and inexpensive; today's user-oriented software is easier to handle by non-experts, thus widening the potential spectrum of application in architectural and archaeological recording.

Thanks to its simplicity, image rectification remains the most popular method in this field for both photogrammetrists and users. But when object anaglyph exceeds the tolerances of planarity, stereo or multi-image configurations need to be considered. Notwithstanding the merits of commercial software packages for relatively simple work in close-range, the use of more images at a time does not appeal to non-expert users but also raises cost; besides, the point-wise reduction schemes are basically adequate only for objects consisting of planes (for instance, continuous non-straight lines such as the outlines of a curved wall-stone cannot be mapped). Of course, complications and requirements in instrumentation grow rapidly once stereoviewing is introduced.

Thus, it is expedient to go beyond the limitation of near-planarity (posed by rectification) by exhausting the potential of 'monoplotting'. Its application to irregularly shaped surfaces requires a digital elevation model (DEM). Contrary to aerial mapping tasks where ground DEMs may already be at hand from previous work, in terrestrial applications DEMs have first to be created. But – 'halfway' between flatness and irregular relief – smooth surfaces which may be approximated analytically are often to be met in close-range applications. Among these, quadrics are most widely encountered: cylindrical, spherical, conic or parabolic analytical surfaces are suitable for partly, or fully, describing shape for a variety of ancient theatres or tombs and also churches, monasteries, towers, rotundas, domes, cupolas, vaults, ceilings, mills, lighthouses, factories, aqueducts, chimneys etc. (to which several industrial objects may be added).

On the one hand, the need for geometric shape-fitting to 3D data is now situated within the context of the growing use of CAD systems (Chandler & Cooper, 1991); on the other, second order surface fitting to points sampled by photogrammetry has been employed to establish theoretical shape and check discprepancies (Feltham, 1990; Fotiou et al., 1991) as well as for mapping and orthophoto production tasks (Restle & Stephani, 1988). Questions of 'flattening' non-developable surfaces, e.g. spherical, have also been addressed (Vozikis, 1979).

In this contribution, the basic idea lies in the recognition that known analytical surfaces provide the missing third equation supplementing the collinearity condition, hence permitting mapping from single images. Unlike conventional monoplotting, this procedure is direct (non-iterative). However, certain questions regarding non-uniqeness of solution have to be answered. In the case of a developable surface, monoplotting can further result in unwinded vector data. In fact, for such objects not only the generation of orthoimages is possible; digital 'unwrapping' of the original imagery and subsequent mosaicking may also be performed with simple means and suitable software. In this manner, full all-around development retaining all the wealth of the original raster data may be generated. Here, the underlying concept is exemplified by the case of right circular cylinders but may well be accordingly extended to the other analytical surfaces.

2. ANALYTICAL SURFACE FITTING

The best-fitting analytic expression of a quadric surface is determined either directly (in the simple cylindrical case a perimeter suffices) or by fitting to redundant points measured geodetically or photogrammetrically. A distinction is made between cases where surface type is given or 'obvious' and its specific equation is to be found; and instances where the surface type is not assumed beforehand.

In this last case the full second order equation of nine independant unknowns is fitted to the 3D point set. General-

ly, these coefficients in fact correspond to the three parameters of the canonical form defining shape (i. e. surface type) and size; and the six elements of rigid body transformation fixing surface position and orientation in the coordinate system. Restle & Stephani (1988) outlined steps for detecting rotatory surfaces, classification and extracting canonical forms from the full second degree equation.

On the other hand, assumption of specific surface types allows to directly use their corresponding general equations. For a right circular cylindrical surface, in particular, different models have been given (Feltham, 1990; Chandler & Cooper, 1991). In fact, the independent parameters of this solid are just five (as also pointed out by Robson et al., 1992). The physical meaning is as follows: radius R suffices for fixing its canonical form; it has only four degrees of freedom in space as translation along and rotation about its axis ĩ does not affect it. Or, put otherwise, a right circular cylinder is fully known through four elements that fix its axis ξ as a straight line in 3D space and the common distance (R) of all its points from ξ.

Indeed, among the three XYZ coordinates fixing an arbitrary point K of a line and the three direction numbers L, M, N defining its direction two corresponding constraints must be imposed. Amongst possible constraints (Petsa, 1996) and provided that axis orientation is even vaguely known, it is simplest to set K as belonging to one of the XY, YZ or ZX planes and to set one (non-zero) direction number equal to unity. For a cylinder whose axis is not parallell, say, to the YZ plane, the constraints then are: $X_K = 0$, $L = 1$. These can be directly introduced into the condition equation employed for surface approximation. This may equivalently be: either the equation yielding the distance of a point from a line; or an equation of a circle on, say, the Y′Z′ plane made perpendicular to the cylinder axis ξ via two rotations which are functions of its direction numbers. In the example of the above two constraints, for instance, the condition used for fitting finally becomes:

$$\begin{aligned} &X^2(M^2+N^2)+(Y-Y_K)^2(1+N^2)+(Z-Z_K)^2(1+M^2)- \\ &-2X(Y-Y_K)M-2X(Z-Z_K)N-2(Y-Y_K)(Z-Z_K)MN- \\ &-R^2(1+M^2+N^2)=0 \end{aligned} \qquad \textbf{(1)}$$

with the five unknowns R, Y_K, Z_K, M, N which are solved for in an iterative adjustment process. Initial values may be found from two points approximately defining a generating line. This model has been tested in other cases but not the test object mentioned later whose axis is vertical.

3. DIGITAL MONOPLOTTING

3.1 Basic Equations

With known interior and exterior camera orientations, the analytic equation of the surface provides a third condition supplementing the two conventional collinearity equations – or the direct linear transformation equations (DLT) – for each image point q(x,y). Hence, space intersection of the single projective ray ĩ, passing through projective centre O and q, with the surface results in the 3D coordinates of digitized image points (Figure 1). If the camera constant c is unknown, for most practical purposes an approximate value could be used in space resection and thereafter due to small object depth. The control points used for exterior orientation should preferably be six for each photograph (each three will also appear on the neighbouring images).

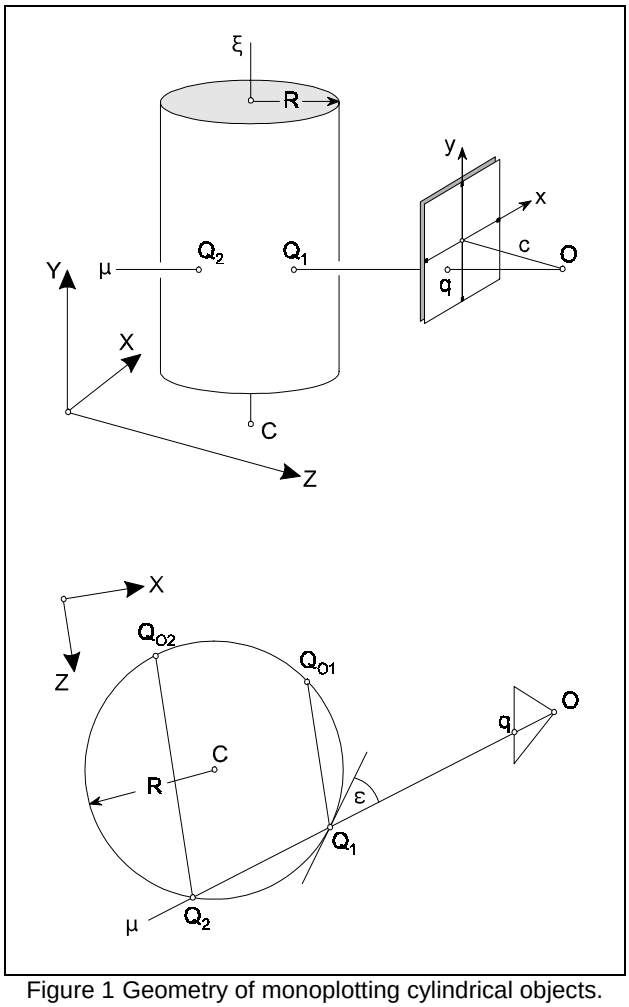

Figure 1 Geometry of monoplotting cylindrical objects.

The process is simpler if space data are transformed to a cylinder-centered system XYZ by means of two rotations resulting, for instance, in ξ // Y (as in Figure 1); shift of the origin to the intersection point C of ξ with the XZ plane will then lead to ξ ≡ Y. The two collinearity equations can be written in the form

$$X = uZ + U \qquad Y = vZ + V \qquad \textbf{(2)}$$

whereby u, v are functions of the image coordinates (x,y), interior orientation elements (c, x_o, y_o) and the image rotations (ω,φ,κ) while U, V also depend on the perspective centre location (X_o, Y_o, Z_o). Combination of the squared X–equation with that of a circle now describing the cylinder in the new system gives:

$$Z^2 = \frac{X^2 + U^2 - 2UX}{u^2} = R^2 - X^2 \qquad \textbf{(3)}$$

from which X is finally solved for as

$$X_{1,2} = \frac{U \pm u\sqrt{(1+u^2)R^2 - U^2}}{1+u^2} \qquad \textbf{(4)}$$

Introduced into the circle equation, each of roots $X_{1,2}$ provides two Z–values; each of these results in one Y–value from the second of Eq. 2. The consequence is that a total of four points Q_1, Q_{o1}, Q_2, Q_{o2} are generally obtained, as illustrated in Figure 1. It is $X_1 = X_2$ once a projective ray μ

either is parallel to the X–axis when projected on the XZ–plane, whence $Q_1 \equiv Q_{o1}$, $Q_2 \equiv Q_{o2}$, or is tangential to the cylinder (one solution) which is of no practical interest.

3.2 Investigation

Among the four solutions, the correct one is automatically selected given the concavity or convexity of the recorded surface. Indeed, as seen from Figure 1, points Q_{o1} and Q_{o2} do not belong to ray μ: they are detected as not satisfying the collinearity equations. If OC > R, then points Q_1 or Q_2 ($OQ_2 > OQ_1$) are retained for convexity or concavity, respectively. Other possibilities – the perspective centre O lies within the cylinder and the imaged part is closer or farther from O than its diametrical, O lies on the cylinder, O ≡ C etc. – can be confronted by the program using the control information available (Theodoropoulou, 1996).

Another aspect of particular interest regards the propagation of image measuring errors $\sigma_{x,y}$ to space coordinates. Important is here the angle ε under which a projective ray μ intersects the surface (Figure 1). This angle decreases rapidly with μ tending towards the tangent. Small angles å cause high uncertainty, especially regarding depth. When planning photography of cylindrical objects one, therefore, needs to fix an accepted ε_{MIN} value and then decide upon imaging distance and total number of images. These parameters also determine the limits of mapping. For given mean photographic scale, narrow or normal angle lenses allow mapping of larger areas than wide angle lenses.

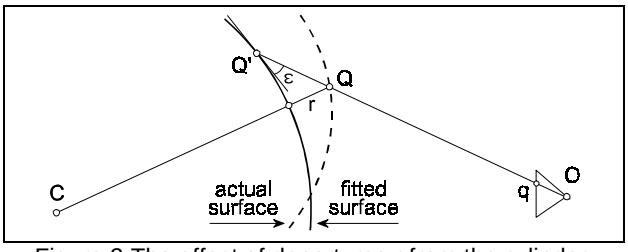

Figure 2 The effect of departures r from the cylinder.

Finally, a last point to be made regards errors introduced into monoplotting due to radial departures r of the actual surface from its best-fitting analytical solid. In Figure 2 it is shown that, although image point q corresponds to actual point Q, it is a point Q′ on the fitted solid which is mapped instead. Spatial displacements QQ′ depend on departures r and angle ε. According to the residuals of fitting and the required accuracy, this consideration could further restrict the useful area of mapping from each single image.

3.3 Implementation

The basic steps of monoplotting cylindrical surfaces may be summarized as follows:

1. Fitting of the analytical solid to sparce XYZ data.
2. Transformation of 3D data to cylinder-centred system.
3. Space resection using appropriate control points.
4. Manual tracing of image vector detail (x, y).
5. Space intersection of projective rays with the analytical surface resulting in 3D vector data.
6. Merging of data from all images for the whole object.
7. Development of 3D vector data in suitable projection.
8. Representation in 3D and 2D.

In the adopted cylinder-centred XYZ system developing is simplest in a 2D system X_D,Y_D with $X_{Di} = \alpha_i R$, $Y_{Di} = Y_i$, in which α_i ($0 \le \alpha_i < 2\pi$) denotes the angle formed by each individual radius CQ_i and the positive Z–axis.

4. DIGITAL UNWRAPPING OF ORIGINAL IMAGES

The second approach introduced here provides the final product not in vector but in raster form. It is based on the fact that a known analytic surface is practically equivalent to a surface DEM. Thus, production of digital orthoimages of the solid is now conveniently possible. Generally, however, the conventional orthoimaging of curved surfaces of architectural or archaeological interest does not fully meet the requirements of the user. In these cases, and for developable surfaces in particular, it is an unwrapping of the surface in question which is basically desirable. Evidently, such photographic (raster) object presentations cannot be directly based on conventional DEMs but rather on 'DDMs' (digital development models), namely planar (X_D,Y_D) grids uniquely referenced to the actual surface (Vozikis,1979).

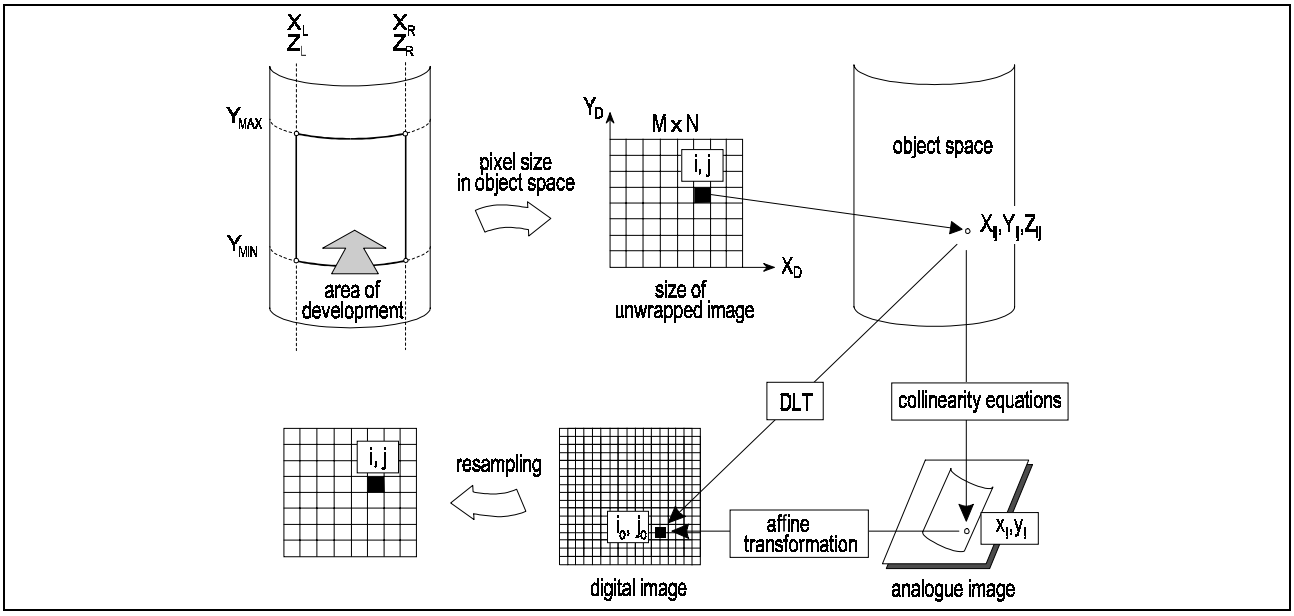

Figure 3 The basic phases of digital unwrapping of right circular cylinders.

This procedure of digital 'photo-unwrapping' is realized in following phases which are also illustrated in Figure 3.

1. For each image the area of development is fixed by its left $(X,Y)_L$ and right $(X,Y)_R$ points, and Y_{MIN}, Y_{MAX}.
2. Next, the system X_D,Y_D of development is established with known correspondences $(XYZ) \leftrightarrow (X_D,Y_D)$.
3. The pixel size in developed object space is chosen.
4. Hence, the size $M \times N$ of the unwrapped image is fixed.
5. For each elementary patch i,j of the unwrapped image the object space coordinate $(X,Y,Z)_{ij}$ is found.
6. Back projection through the collinearity condition leads to the corresponding point $(x,y)_{ij}$ on the film plane.
7. The corresponding position i_o,j_o on the scanned image is established with affine transformation.
8. Alternatively, the last two steps are fused into one by a direct linear transformation between scanned image and object space.
9. From i_o,j_o the grey value of pixel i,j of the unwrapped image is interpolated.
10. Finally, resampled images are adapted radiometrically and combined into a single mosaic to provide a raster end product of surface development.

Figure 4 Two images of the water-tower.

5. APPLICATION

5.1 Test object and data acquisition

A late 19th-century railroad water-tower (right circular cylinder of R = 1.25 m, height 2.5 m; cap radius 1.35 m) was fully covered with 6 images of negative scale 1:120, taken with an amateur 35 mm camera (f = 70 mm); they were enlarged ×4 and scanned at 350 dpi (two images are in Figure 4). To the total of 24 control points (σ = 1.4 cm) a circle on the XZ–plane was fitted (centre: $\sigma_{X,Z}$ = 0.5 cm; σ_R = 0.4 cm). Digital images and object space were related to each other directly with the DLT–approach via 7–9 control points per image (Theodoropoulou, 1996).

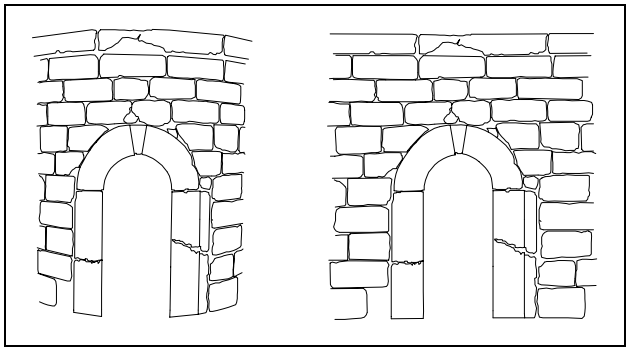

Figure 5 Perpsective and developed part of an image.

5.2 Vector development

Manual digitization of all scanned images was performed within the Autocad 12 environment through the RASTEREX RxAutoIcon–P software. Exported DXF files containing all perspective vector information were then used to transform digitzed image data to corresponding 3D polygons on the cylinder surface; these were subsequently developed. The cap was separately transformed with its own radius.

Figure 5 shows the original perspectively distorted data from an image and the developed vector product. All separate unwindings were finally merged to generate – after some editing – the full development of the water-tower as seen in Figure 6. The RMS differences in the final position of the control points was equal to their intitial precision.

5.3 Raster development

All digital images were unwrapped in the described procedure using a pixel size of 5 mm in the 'developed' X_DY_D object space. The cylinder cap was unwrapped separately and inserted into the images at its known height. Image resampling succeeded with a nearest-neighbour interpolation. Figure 7 contrasts an unwrapping to the corresponding orthoimage Radiometric averaging and mosaicking of the new images were performed using a commercial software (ADOBE Photoshop 2.5). The full mosaic is shown in Figure 8.

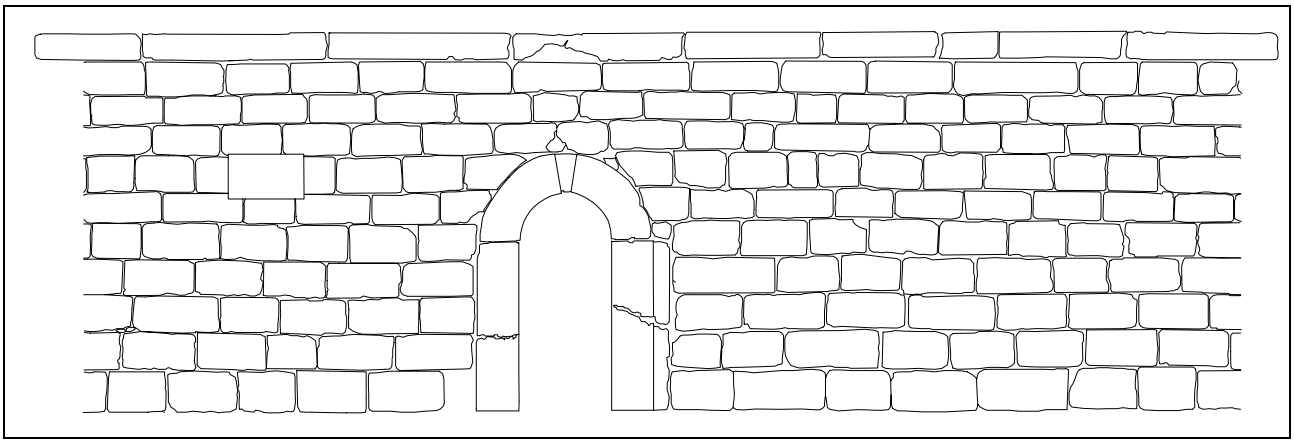

Figure 6 Full view of merged vector data after development.

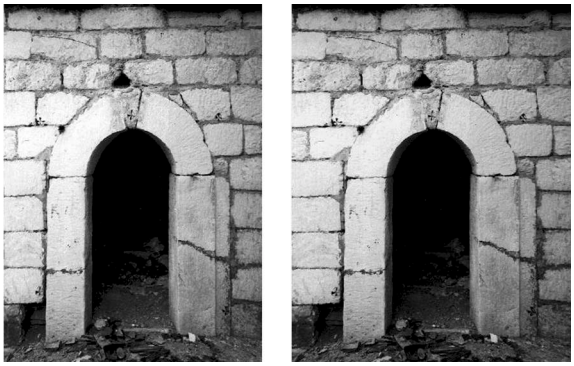

Figure 7 Orthoimage and unwrapped image.

The RMS differences of similarity transformation between mosaic and control points in $X_D Y_D$ object space were 2.8 pixel (= 1.4 cm) in the direction of development and 0.9 pixel (= 0.5 cm) in height.

6. CONCLUSION

An approach has been formulated for mapping 3D objects of regular shape, to which it is possible to fit mathematical surfaces, from single images. In case the solid is developable, it has been demonstrated that besides vector data one may also perform digital 'unwrapping' and mosaicking of the original images.

Here, the right circular cylinder has been investigated and tested in practice. It was seen that the accuracy of object space coordinates depends essentially on the angle under which projective rays meet the surface. Mapping limits for each image should be fixed accordingly; control has to be reliable and well distributed.

The photogrammetric methods being currently applied in architecture range from the simplest to very sophisticated ones. It is believed, however, that the less demanding is a method in its use the more it may encourage users to recognize the merits of digital close-range photogrammetry.

In this context, the presented method is being introduced into the digital rectification software DIRECT (reported by Patias, 1991, and subsequently extended by Karras et al., 1993, to function also with vanishing points rather than control points). This contribution represents a further step towards fully exhausting the potential of monoscopic and monoplotting techniques for the purposes of architectural and archaeological documentation.

Figure 8 Full mosaic of the digitally unwrapped images

REFERENCES

Chandler, J.H., Cooper, M.A.R., 1991. Determining cylindrical parameters – an alternative approach. Land and Hydrographic Survey, September, pp. 5-7.

Feltham, R.M., 1990. Determining cylindrical parameters. The Photogrammetric Record, 13(75), pp. 407-414.

Fotiou, A., Livieratos, E., Lombardini, G., Paraschakis, I., 1991. Dome representation using photogrametric data and best fitting techniques. ISPRS Journal of Photogrammetry & Remote Sensing, 46, pp. 231-326.

Karras, G.E., Patias, P., Petsa, E., 1993. Experience with rectification of non-metric digital images when ground control is not available. Proc. XV International CIPA Symposium, Bucarest. [In print.]

Patias, P., 1991. Architectural photogrammetry goes to the digital darkroom. XIV CIPA Symposium, Delphi, pp. 129-139.

Petsa, E., 1996. Line Photogrammetry. Ph.D. thesis, De - partment of Surveying, N.T.U.A. [In Greek.]

Restle, M., Stephani, M., 1988. Derivation of surfaces of second order degree from photogrammetric measurements for orthophoto production. Proc. XI International CIPA Symposium, Sofia, pp. 194-205.

Robson, S., Parbery, R.D., Fryer, J.G., 1992. Analysis of as-built cylindrical shapes. The Australian Journal of Geodesy, Photogrammetry and Surveying, 56, pp. 91-109.

Theodoropoulou, I., 1996. Digital Monoplotting of Cylindrical Objects. Diploma thesis, Dept. of Surveying, N.T.U.A.

Vozikis, E., 1979. Die photogrammetrische Differenzialumbildung gekrümmter Flächen mit Beispielen aus der Architekturbildmessung Institut f. Photogrammetrie, Geowissenschaftliche Mitteilungen Nr. 17, T. U. Wien.